Synoptic Connections and Impacts of 14-Day Extreme Precipitation Events in the United States

MELANIE SCHROERS[a] AND ELINOR MARTIN[a,b]

[a] *School of Meteorology, University of Oklahoma, Norman, Oklahoma*
[b] *South Central Climate Adaptation Science Center, Norman, Oklahoma*

(Manuscript received 26 August 2021, in final form 5 April 2022)

ABSTRACT: Long periods of extreme precipitation can cause costly damages to a region's infrastructure while also creating a higher risk for the region's population. Planning for these periods would ideally begin at the subseasonal-to-seasonal time scale, yet prediction of precipitation at this time scale has low skill. In this study, we will use Jennrich et al.'s database of 14-day extreme precipitation events to understand more about the synoptic connections and impacts of these extended extreme events. The synoptic connections of events were examined using the composites of event-day 500-hPa geopotential height and precipitable water anomalies. The combination of these two drivers leads to higher skill in the West Coast and Great Lakes than other regions, with an equitable threat score of 0.137 and 0.084, respectively, and higher conditional probabilities of event occurrence. Therefore, the synoptic patterns associated with events, although significant, are not unique, which poses prediction challenges. Historical impacts of these events, using NCEI storm reports, were assessed to benefit decision-makers in future risk mitigation. A variety of reports were found during events, from winter weather reports in West Coast events to tropical storm reports in Southeast events. Every region has significantly more flooding reports during events than in nonextreme 14-day periods, demonstrating the impacts of such extended events. Although there is still much to learn about extreme precipitation events, this study contributes to the foundational knowledge of synoptic drivers and impacts of events.

KEYWORDS: North America; Extreme events; Precipitation; Climate prediction; Societal impacts

1. Introduction

Bridging the gap between daily forecasting and seasonal prediction has become an increasingly important topic in order to improve risk mitigation for decision-makers. The World Climate Research Programme created an initiative to improve prediction at the subseasonal-to-seasonal time frame (S2S), meaning two weeks to three months in advance, with one focus area being the prediction of climate extremes (Robertson et al. 2015). Impacts from extreme precipitation may be felt in multiple sectors including infrastructure, agriculture, water management, transportation, and health (e.g., Curriero et al. 2001). Impact mitigation efforts made by decision-makers for extreme precipitation events may take several weeks to implement, yet S2S forecast skill is low when compared with daily forecasts (1–10 days) or seasonal forecasts (3+ months), in part because of lack of understanding of the drivers of S2S extremes (Vitart et al. 2017; Brunet et al. 2010). Pan et al. (2019) showed that S2S hindcast products, from the S2S prediction project, provide no additional skill within wintertime West Coast precipitation, while Sharma et al. (2017) found that precipitation hindcasts, from NCEP Global Ensemble Forecast System Reforecast (GEFSRv2), tend to have an underforecasting bias and low skill past a 7-day lead time within the eastern United States. However, other large-scale variables have been shown to have greater skill at longer lead times (Son et al. 2020). Studies of the prediction of extreme precipitation within the Mediterranean Sea region and the United Kingdom found that using large-scale variables may improve lead times (Mastrantonas et al. 2022; Richardson et al. 2020). Therefore, synoptic connections of 14-day extreme precipitation events within the CONUS could be a favorable proxy for future prediction at the S2S time scale.

To have reliable predictions of 14-day events across the CONUS, the drivers of these events must be investigated. Yet, there are very few studies that investigate longer time frame precipitation across the entire CONUS with a consistent definition of extreme. Many studies focus on extreme precipitation on daily, seasonal, or yearly time scales, leaving S2S time scales with little examination (Barlow et al. 2019). At daily time scale, it has been found that precipitation has been increasing over the past century, mainly due to the positive trend of extreme daily precipitation (Karl and Knight 1998; Kunkel et al. 1999; Groisman et al. 2012). There are regional based analyses of daily precipitation events across the CONUS (e.g., Zhao et al. 2017; Schumacher and Johnson 2006; Groisman et al. 2012), as well as regional yearly precipitation analysis (e.g., Flanagan et al. 2018). Case studies of extended precipitation events have been conducted to look into the drivers of the flooding that occurred within the regions (e.g., Furl et al. 2018; Kunkel et al. 1994). Furl et al. (2018) found that during the southern Great Plains flooding event in May of 2015 there was a large amount of precipitable water before the onset of the event that was consistently being resupplied from the Gulf of Mexico. Kunkel et al. (1994) studied

Supplemental information related to this paper is available at the Journals Online website: https://doi.org/10.1175/JAMC-D-21-0174.s1.

Corresponding author: Melanie Schroers, maschroers@ou.edu

DOI: 10.1175/JAMC-D-21-0174.1

the 1993 summer flood of the Upper Mississippi River basin. The persistent rainfall throughout the region from June to August occurred as a result of below-normal 500-hPa geopotential heights over the Rocky Mountains and above-normal heights over the eastern United States. During this event they also experienced above-normal soil moisture and below-normal evaporation that led to devastating flooding through the region.

To have a consistent definition of 14-day precipitation events, Jennrich et al. (2020) created a database of 14-day extreme precipitation events for six regions across the CONUS from 1981 to 2010. The synoptic characteristics of these events vary depending on the region. All regions show a distinct 500-hPa height anomaly dipole within the extreme event composites, oriented differently in each region, as well as an anomalous increase in 200-hPa zonal winds and moisture flux into the respective region. Understanding how often these anomalous patterns show up during events or nonevents will help to understand the strength of the synoptic connections for these events so that decision-makers are more equipped into the future.

In 2018, as part of the larger Prediction of Rainfall Extremes at Subseasonal to Seasonal Periods project (PRES^{2}iP), a workshop was held with 22 decision-makers, including emergency mangers, water resource managers, and tribal environmental professionals, from across the United States. The goal of the workshop was to learn what mattered most to those who use, and rely on, predictions of extreme rainfall (VanBuskirk et al. 2021). From this workshop, we learned that decision-makers start planning two weeks to two months before an event and make final decisions when closer to the start of the event. When asked how to define an extreme precipitation event, there were widely varying definitions, with many answers referencing the difference between an extreme event and extreme precipitation. Although there might be extreme precipitation, this might not always result in an extreme event with many impacts (VanBuskirk et al. 2021). Therefore, it is important to analyze impacts associated with extreme precipitation for stakeholder to trust that events of interest to scientists are relevant for them.

Miller et al. (2008) found that flooding is the costliest of all natural disasters and therefore is of particular interest in the case of 14-day precipitation events. Flooding also affects the most people and occurs the most often when compared with other weather-related disasters (United Nations 2015; Slater and Villarini 2016). For example, during the event in May 2015 within the southern Great Plains, studied by Furl et al. (2018), there was a total of $2.8 billion of damage, with 31 fatalities (NCEI 2019). This was caused by the widespread rain that had already occurred earlier in the month that created runoff conditions within the Blanco River basin. Although 14-day extreme events happen less frequently than daily extreme rainfall, they can result in devastating damages that may take multiple years to fully recover from and therefore merit a more thorough understanding. Hence, the objectives of this study are to survey the impacts of the 14-day extreme precipitation events defined by Jennrich et al. (2020), as well as examine the synoptic connections of these events by investigating how often the synoptic patterns found from compositing are associated with events or nonevents.

2. Data and methods

a. Observations and reanalysis

Precipitation data from the Parameter–Elevation Regression on Independent Slopes Model (PRISM) were utilized to define 14-day extreme precipitation events throughout seven regions in the CONUS from 1981 to 2018, defined in section 2b. PRISM interpolated many point observations onto a 4-km grid (PRISM Climate Group 2004). This interpolation process uses elevation and weighted station measurements to find estimates in areas with no direct observations (Daly et al. 2008). PRISM precipitation was chosen after comparing event dates for multiple precipitation datasets: Livneh (0.0625° resolution, from 1915 to 2011), ERA5 reanalysis precipitation (30-km resolution, from 1979 to present), and ERA5 that was regridded, by bilinear interpolation, onto a 1° resolution grid (Livneh et al. 2013; Copernicus Climate Change Service 2017). All four datasets found similar events throughout 1981–2010; thus, PRISM was chosen because of its high resolution and for consistency with Jennrich et al. (2020).

The European Centre for Medium-Range Forecasts ERA5 reanalysis was used for all large-scale variables, including 500-hPa geopotential height and precipitable water (Copernicus Climate Change Service 2017). ERA5 variables have an hourly temporal resolution at a spatial resolution of 0.25°, with 137 vertical levels up to 1 hPa. Hourly data were averaged into daily values for the studied period.

b. Extreme definition

Jennrich et al. (2020) created a database of 14-day extreme precipitation events in six regions within the continental United States using PRISM precipitation from 1981 to 2010. Regions used in Jennrich et al. (2020) include the Great Plains, Great Lakes (GL), Northeast (NE), Southeast (SE), Mountain West (MW), and West Coast (WC). Flanagan et al. (2018) found that long-term precipitation drivers differ from the northern Great Plains to the southern Great Plains. Therefore, in this study, seven regions were used by splitting the Great Plains into the North Plains (NP) and South Plains (SP). Spatial distribution of the extreme events within the seven regions can be seen in Fig. 1.

The 14-day extreme events were defined, following Jennrich et al. (2020), by using a set of criteria for a 14-day sliding window from 1981 to 2018 for seven regions:

- precipitation at each grid point is defined as extreme using the 95th-percentile threshold of 14-day total precipitation,
- total area of extreme precipitation during the 14-day sliding window must exceed a specific threshold, as summarized for each region in Table 1,
- if the number of days with area-averaged precipitation above 10 mm day^{-1} is less than 5 days (or 3 days in MW) the 14-day window is excluded,
- the heaviest precipitation day and the surrounding two days cannot exceed 50% of the 14-day total precipitation, and

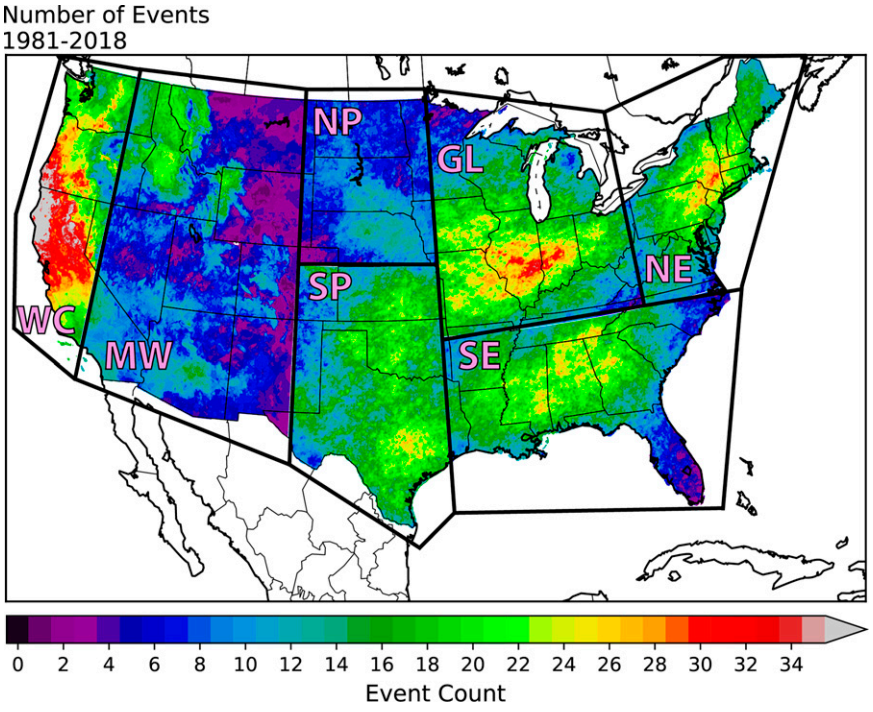

FIG. 1. Event counts of 14-day extreme events for seven regions across the CONUS from 1981 to 2018 using PRISM precipitation. Shown are the seven regions in which 14-day extreme events are found: Northeast (NE), Great Lakes (GL), Southeast (SE), South Plains (SP), North Plains (NP), Mountain West (MW), and the West Coast (WC).

- if two events are found that are overlapping, the event with the highest precipitation totals is kept.

To investigate seasonality of events, the wet and dry seasons were defined by a regional principal component analysis on monthly mean precipitation. The leading mode, which explains nearly all of the variance, represents the region's precipitation monthly seasonality with the principal component being positive in the wet season and negative in the dry season. A summary of the regions can be found in Table 1, including thresholds used, the total number of events, and regional precipitation seasonality. Further details, including sensitivity to criteria, can be found in Jennrich et al. (2020).

TABLE 1. Information on the seven regions used to classify our events.

Region	Abbreviations	Total events	Area threshold (km^2)	Wet season
Northeast	NE	38	200 000	Apr–Oct
Southeast	SE	46	300 000	All year
Great Lakes	GL	54	300 000	Apr–Sep
Northern Plains	NP	17	200 000	Apr–Sep
Southern Plains	SP	57	200 000	Apr–Oct
Mountain West	MW	50	200 000	Nov–May
West Coast	WC	51	200 000	Oct–Apr

c. *Synoptic connections methods*

The synoptic connections of regional events were found by comparing the composite of standardized 500-hPa geopotential height or standardized precipitable water anomalies from the 14-day precipitation events with composites of standardized anomalies of the variables of a 14-day sliding window from 1981 to 2018. A CONUS-wide domain of 15°–65°N and 150°–50°W was used for the height composites (e.g., Fig. 4a), while a smaller regional domain was used for the precipitable water composites (e.g., Fig. 4b). Small changes to the domains did not result in differences in skill (not shown). Compositing event variables based on whether they occurred in the wet or dry season resulted in similar composites found for all event days. Comparison between regional event composites and the composites of the 14-day periods was conducted by finding the congruence coefficient (CC) for all 14-day periods:

$$\mathrm{CC} = \frac{\sum X_{\mathrm{event}} Y_{\mathrm{window}}}{\sqrt{\sum X_{\mathrm{event}}^2 \sum Y_{\mathrm{window}}^2}}, \tag{1}$$

where X_{event} is the extreme event composite and Y_{window} is the sliding window of 14-day standardized anomalies composite. If any 14-day sliding window begins with an event day (i.e., one of the days identified as an extreme 14-day event in section 2b), it is considered to be an event period; therefore, there are 14 event periods for one given extreme event. Any sliding window that does not begin with an event day is

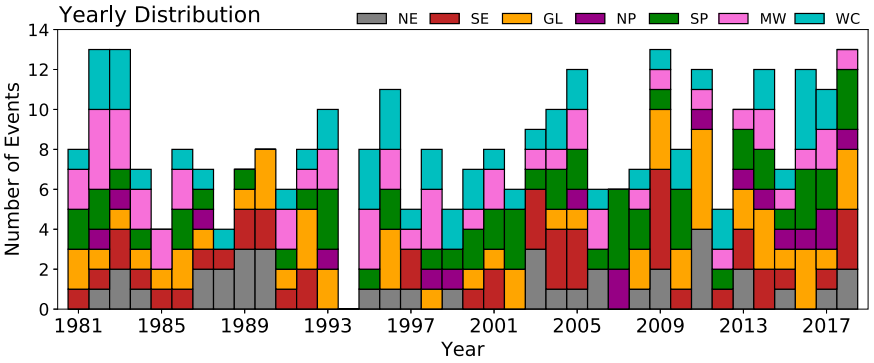

FIG. 2. Distribution of 14-day extreme precipitation events, from 1981 to 2018, by year for all seven regions (colors).

considered to be a nonevent period. Utilizing this definition of event and nonevent periods generally provided the highest skill, as well as a greater sample size, when compared with other definitions. The skill distribution with changing lagged sliding window start dates is shown in Fig. S1 in the online supplemental material. This maximum in skill, at lag zero, may relate to how the synoptic patterns, seen within the event composites, develop or strengthen in relation to the events.

A threshold of CC of 0.35 was used to discern between similar and nonsimilar synoptic patterns. Fourteen-day periods with a CC above this threshold, for each region, were found to have similar synoptic patterns when compared with the regions' event-day composites. Increasing the CC threshold from 0.3 to 0.5 resulted in small or no change in skill (not shown). For each region, the conditional probabilities of the occurrence of an event, given that the period was above or below the threshold were found, similar to Mastrantonas et al. (2022):

$$P(\text{event}|\text{above}) = \frac{\text{Event periods above/equal 0.35}}{\text{All periods above/equal 0.35}} \quad \text{and} \tag{2}$$

$$P(\text{event}|\text{below}) = \frac{\text{Event periods below 0.35}}{\text{All periods below 0.35}}. \tag{3}$$

This probability indicates how often our extreme event composites were seen in event or nonevent periods. Conditional probabilities can then be compared with the climatological base rate of event days within a region (seen as base rate in Table 3). Assessment of skill was conducted using the equitable threat score [ETS; see Eq. (S1) in the online supplemental material]. This skill metric has a range from $-1/3$ to 1, where 0 indicates no skill.

d. Impacts

The National Centers for Environmental Information (NCEI) storm events database was utilized to understand the storm-related impacts for events that took place after 1996 (NCEI 2020). Previous to 1996, only reports of tornado, thunderstorm wind and hail were documented by the storm prediction center. After 1996, 48 event types, detailed in Murphy (2018), were recorded into the storm events database. Every report was recorded on the basis of the county of occurrence by a National Weather Service forecast office and then passed onto NCEI. Because of regional reporting, some report types have multiple definitions. For example, the amount of precipitation that may result in a flood report in the MW may not result in a flood report in the SP because of the regional differences of precipitation. Storm reports seen during the all 14-day events were split into the seven regions by nearest state boundaries because of county-based reporting. For each region, reports that have more than 100 occurrences during all events were summarized. Flood, flash flood, and heavy rainfall storm reports were of particular interest for our extreme rainfall events. These reports are all indicative of loss of life or property from excessive precipitation (Murphy 2018). The regional distributions of report totals for flood, flash flood, and heavy rain were found for all 14-day extreme events, as well as for 1000 random 14-day periods, excluding event days, from 1996 to 2018. These distributions were then tested for significant difference using a permutation test with 1000 iterations at a $p < 0.1$ level. Although storm reports do not give the exact impacts that may be experienced on the ground, they can assist with overall risk. Knowing the typical storm reports of extreme precipitation events, can help decision-makers know what impacts may occur during the events.

3. Results

a. Summary of events

The extension of Jennrich et al. (2020) to 2018 did not alter the overall climatology of events. However, splitting the plains into the NP and SP resulted in many more events in the SP, with a total of 57 events, than in the NP, with a total of 17 events (Table 1). Most of the NP events are seen at the end of the time frame, with 8 of 17 occurring after 2010, as seen in Fig. 2. When looking at all events, across all regions, from 2011 to 2018, there are six years that have at least 10 events or more, whereas in the previous 30 years there are only seven years that have 10 events or more. The monthly distribution of events per region also matches closely with what was found in Jennrich et al. (2020). The GL, NP, and SP

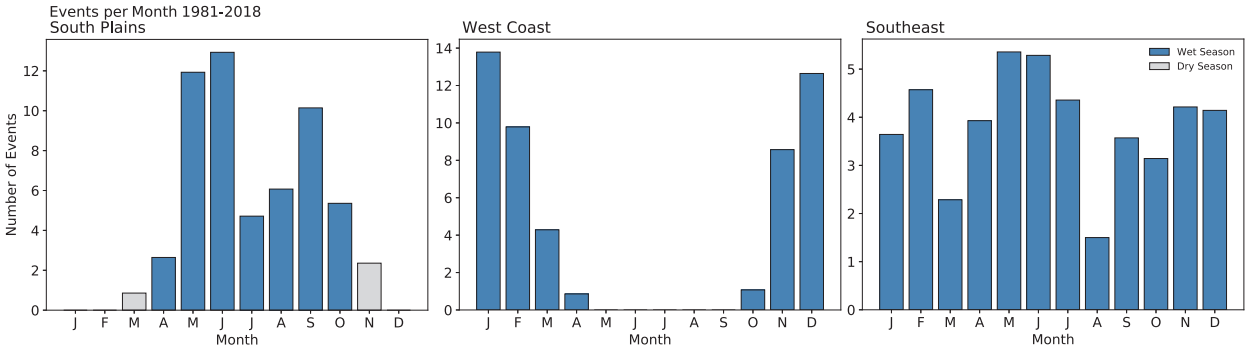

FIG. 3. Number of extreme events per month in the (left) SP, (center) WC, and (right) SE from 1981 to 2018. Wet-season events are blue, and dry-season events are gray. (Note that the *y* axis has different limits for each region.)

have a bimodal distribution with maximums in June and early autumn, just as seen as in the GL and the Great Plains in Jennrich et al. (2020) (Fig. 3 and Fig. S2). These maximums occur during the typical wet seasons of the regions, with only a few events occurring within the dry season. By contrast, the NE and SE had events throughout the entire year. The WC and MW events occurred within the winter months, during their typical wet seasons, seen in Fig. 3 for the SP, SE, and the WC. In the following sections we will discuss the SE, SP, and the WC separately to highlight the similarities and difference between each region. Plots for all other regions are included in the online supplemental material (Fig. S2).

b. Synoptic connections

1) SOUTHEAST

The SE had a total of 46 events, a climatological base rate of event days of 4.6%, from 1981 to 2018. Most events were seen within Mississippi, Alabama, and Georgia, with few events occurring in Florida or around the borders of the region, as seen in Fig. 1. The events occurred throughout the year, given that the SE does not have a distinctive wet season, as seen in Fig. 3. This is consistent with daily precipitation extremes from Schumacher and Johnson (2006) who noted that 24-h precipitation events can occur within any month in the SE. The maximum number of events within the SE is seen during the warm months of May and June, as well as during November–February.

The composite of standardized 500-hPa geopotential height anomalies of all events within the SE can be seen in Fig. 4a. This pattern matches with what was found in Jennrich et al. (2020), despite using different reanalysis data and a longer period, with a statistically significant trough/ridge dipole centered over the region. To investigate how often this geopotential height pattern is seen during events and nonevents, the event composite is compared with all 14-day periods within the time frame. From Tables 2 and 3, we see that 10.0% of the 14-day periods with CC above 0.35 are event periods, whereas only 3.9% of periods below the threshold are event periods. Both of these conditional probabilities are an improvement from the base rate of event days of 4.6%. Despite event periods having larger CCs on average, there are still 1603 nonevent periods above the threshold. This shows very little overall skill in discerning between events and nonevents, with an ETS of 0.044. Geopotential height alone cannot result in precipitation; therefore, precipitable water was also investigated.

The composite of precipitable water during the SE events is seen in Fig. 4b. As expected, we see a large positive standardized anomaly of precipitable water over the SE in the extreme event composite, with values reaching greater than 0.6 for most of the region. The contingency table of all 14-day periods from 1981 to 2018 made from combining CC of all periods' height fields and precipitable water fields is seen in Table 2. The conditional probability of an event occurring when above the 0.35 CC threshold increased from 10.0% to 12.5%. Yet, there are still 505 event periods that do not have similar synoptic conditions. When below the threshold, the probability of an event occurrence increased minimally from 3.9% to 4.0%, this follows given the large amount of nonevent periods below the threshold. Using the drivers together resulted in an increase of ETS to 0.056. Overall, the conditional probability using the event composite patterns provide more skill than the climatological base rate alone, but there are still many missed event periods.

2) SOUTHERN PLAINS

The SP has a total of 57 events, a climatological base rate of event days of 5.8%, the highest event count of all regions. Events occurred throughout the entire region, with more events occurring on the east side of the region, as seen in Fig. 1. There are only six years, from 1981 to 2018, for which the SP did not experience an event. Of particular interest is 2007, which had four events in the SP as well as two events in the NP. While much of the CONUS was in drought, both the SP and NP experienced above-average precipitation throughout 2007 (NCEI 2008).

The composite of standardized 500-hPa geopotential height anomalies of all SP event days from 1981 to 2018 is seen in Fig. 4c. A statistically significant trough/ridge dipole is seen centered over the region. This pattern matches closely in magnitude and location with the height composite for the plains found in Jennrich et al. (2020). This composite has much lower overall magnitudes than any other region's composite,

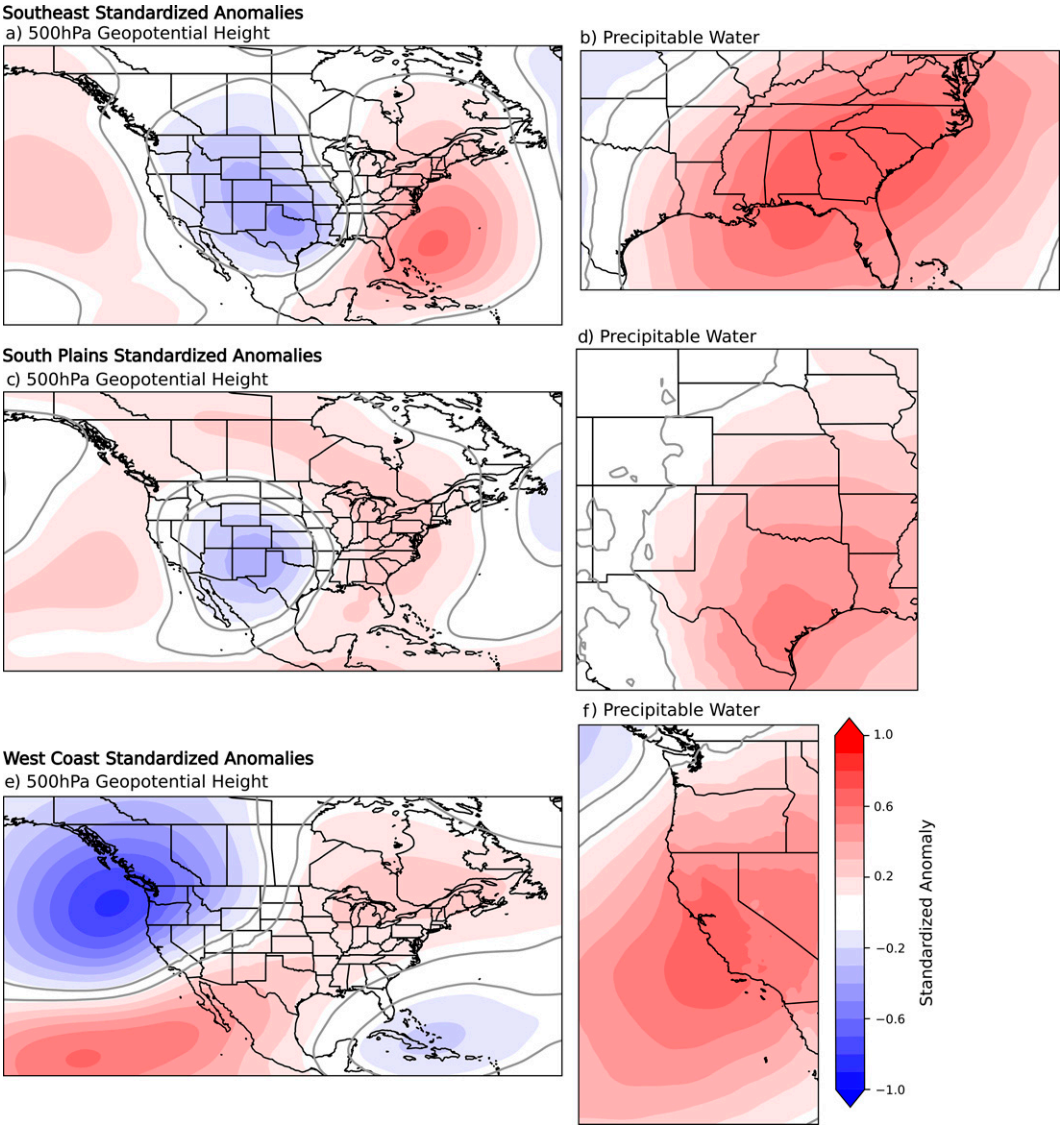

FIG. 4. Composites of all event-day (left) standardized 500-hPa geopotential height anomalies and (right) standardized precipitable water anomalies for the (a),(b) SE; (c),(d) SP; and (e),(f) WC. Significance from a t test at the $p < 0.05$ level is shown as a gray contour.

with values only ranging from −0.4 to 0.3. In comparing this height composite with all 14-day periods in the time period, we found that 11.5% of periods above a CC of 0.35 are considered to be event periods, with a total of 1254 nonevent periods above the threshold (Table 2). Only 5.1% of periods below the threshold are event periods, with 635 missed event periods. Similar to the SE, the conditional probabilities are an improvement from the base rate of event days of 5.8%. This results in an ETS of 0.041. This skill is very similar to what was found in the SE when using geopotential heights alone.

Using the height composite alone to predict SP events resulted in low skill, with a conditional probability of an event period occurring above the threshold of 11.5%. However, when using the composites of geopotential heights and precipitable water together this probability increases. The precipitable water composite of SP events has significant precipitable water anomalies, reaching up to 0.5 for a small portion of the region, near the Gulf of Mexico and throughout most of the eastern portion of the SP (Fig. 4d). Therefore, we want to find periods with anomalous precipitable water throughout the region, with a similar height composite as in Fig. 4. Results are shown in a contingency table in Table 2. We see a small increase in the probability of an event occurring below the threshold from 5.1% with geopotential heights alone to 5.4%. Yet the probability of an event period occurring above the threshold increases from 11.5% to 14.1% as a result of the decrease in the number of nonevent periods above the threshold. Although we do see an improvement with respect to the climatological base rate of 5.8%, the number of event periods above the threshold is only 89. This

TABLE 2. Contingency table for extreme events using CC with 500-hPa geopotential heights (HGTS; first two columns) and heights and precipitable water (HGTs and PW; last two columns) for the SE, SP, and WC. Nonevent periods are all 14-day periods without an event day within the window. The threshold detection of an event is set as a CC of 0.35 or greater.

	HGTS alone		HGTS and PW	
	Event period	Nonevent period	Event period	Nonevent period
SE				
CC ≥ 0.35	179	1603	139	972
CC < 0.35	465	11 610	505	12 241
SP				
CC ≥ 0.35	163	1254	89	542
CC < 0.35	635	11 805	709	12 517
WC				
CC ≥ 0.35	332	1340	215	593
CC < 0.35	381	11 804	498	12 551

shows that many event periods do not have similar patterns to the extreme event composites. Therefore, the overall skill does not improve with the addition of precipitable water within the SP, with an ETS of 0.040.

3) WEST COAST

The WC had 51 total events, a climatological base rate of event days of 5.1%, with most events occurring along the coast, with a maximum in northern California (Fig. 1). Most years within the time frame had at least one event, and only 7 years did not experience an event in the WC. The WC also experiences more events during the boreal winter (December–February) than any other region. This is due to a distinct wet season from October to April. All extreme events in the WC occur during the wet season, with no events occurring from March to September in the time period.

The composite 500-hPa geopotential height of all event days within the WC is oriented differently than other regions but still matches what was found by Jennrich et al. (2020). The composite shows a statistically significant anomaly dipole that is oriented north–south in the eastern Pacific Ocean (Fig. 4e). The trough, with a maximum value of −0.9, is greater in magnitude when compared with the ridge, with a maximum value of 0.7. This synoptic setup would allow for anomalous moisture flux from the Pacific into the region. In comparing this geopotential height composite with the entire time period, we find that 19.9% of 14-day periods above the threshold are event-periods, due to the 332 event periods seen above the threshold. Conversely, only 3.1% of periods below the threshold are event periods, as seen in Table 2. The difference between the two conditional probabilities is the largest of all regions when using geopotential heights alone. It is also the largest improvement from the climatological base rate of event days, with the WC base rate being 5.2%. This highlights that WC events occur with a similar synoptic pattern, as seen within the extreme event composites, more often than events in other regions. Therefore, it follows that the WC has the highest skill, ETS of 0.125, for geopotential heights alone.

Given that the WC had the highest skill with using geopotential heights alone, we can expect comparable results when using both geopotential height and precipitable water. Similar to other regions, the WC precipitable water composite is a large positive anomaly within the region (Fig. 4f). The contingency table for WC events using both height and precipitable water composites is seen in Table 2. The conditional probability of an event occurring above the threshold increases from 19.9% to 26.6%, which shows even greater improvement from the base rate of 5.2%. This is due to the large reduction in nonevent periods that are above the threshold. Therefore, many nonevent periods with similar height composites did not have enough precipitable water to make it over the CC threshold. When looking at periods below the threshold, it is seen that the conditional probability of an event occurring increased minimally from 3.1% to 3.8%, although the number of events below the threshold increased to 498. Because of the reduction of nonevent periods above the threshold skill also increases slightly to an ETS of 0.137.

4) SUMMARY OF ALL REGIONS

All extreme event composites for the seven regions have a 500-hPa geopotential height anomaly dipole, with varying orientations, as well as a positive regional precipitable water anomaly. Extreme event composites from the four regions not discussed above—NE, GL, NP, and MW—can be found in Fig. 5. All 500-hPa geopotential height patterns could lead to rising motion under quasigeostrophic theory that would help enable precipitation to occur. However, these composite

TABLE 3. Summary of the regional event-day base rate, conditional probabilities of an event to occur, given that it is above [*P*(event|above)] or below [*P*(event|below)] the CC threshold of 0.35, and the ETS using 500-hPa geopotential heights alone (HGTS alone), as well as using 500-hPa geopotential heights and precipitable water (HGT and PW) together for all seven regions.

		HGTS alone			HGTS and PW		
	Base rate	*P*(event|above)	*P*(event|below)	ETS	*P*(event|above)	*P*(event|below)	ETS
NE	3.8%	9.7%	3.1%	0.048	11.5%	3.3%	0.052
SE	4.6%	10.0%	3.9%	0.044	12.5%	4.0%	0.056
GL	5.5%	13.7%	3.8%	0.073	17.1%	4.3%	0.084
NP	1.7%	6.6%	1.1%	0.045	7.7%	1.3%	0.051
SP	5.8%	11.5%	5.1%	0.041	14.1%	5.4%	0.040
MW	5.1%	11.7%	4.1%	0.053	16.9%	4.6%	0.057
WC	5.2%	19.9%	3.1%	0.125	26.6%	3.8%	0.137

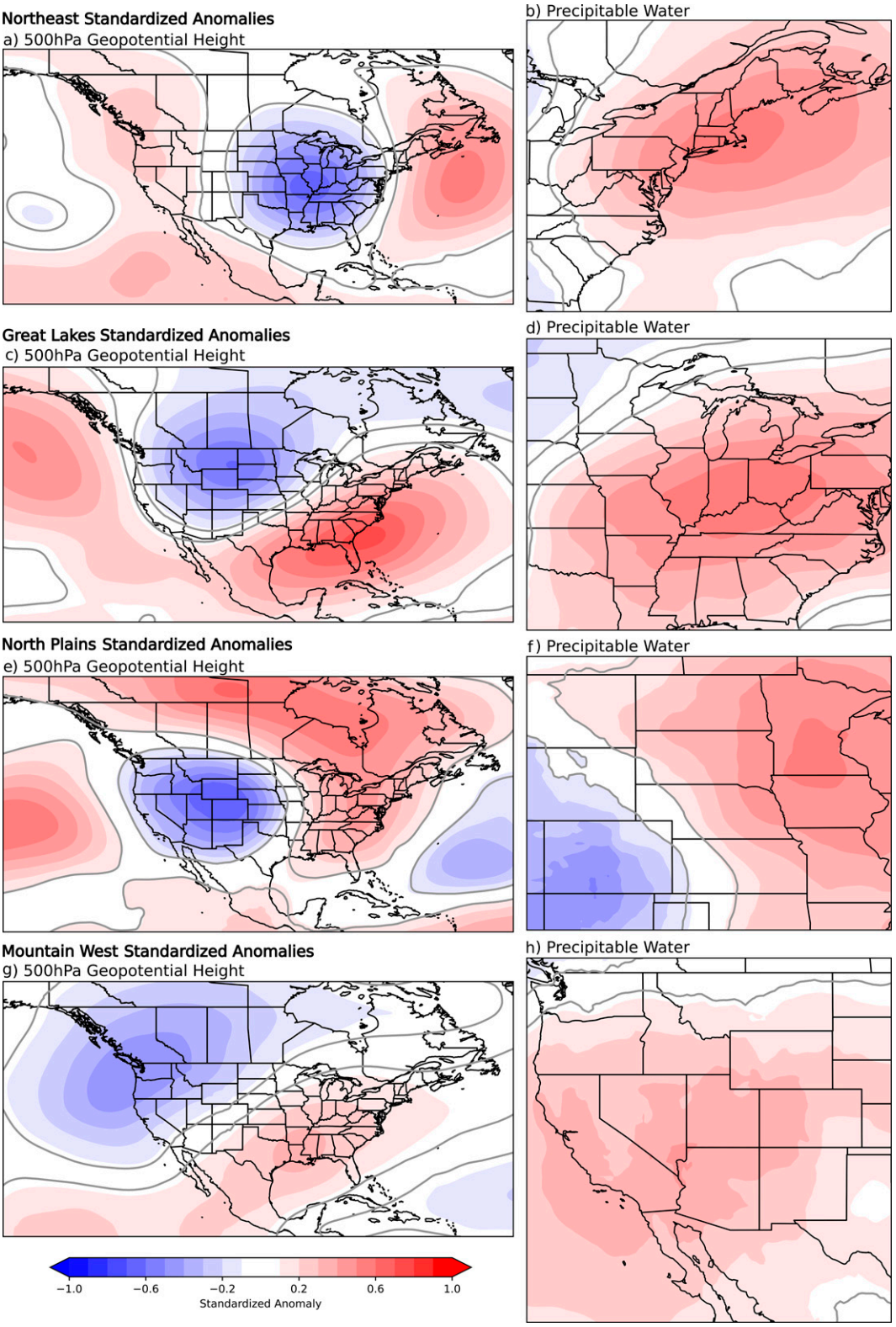

FIG. 5. As in Fig. 4, but for (a),(b) NE; (c),(d) GL; (e),(f) NP; and (g),(h) MW.

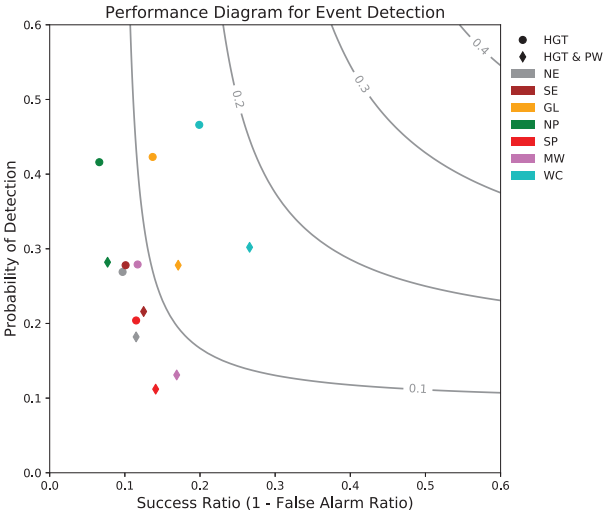

FIG. 6. Performance diagram for event detection when utilizing the events' 500-hPa geopotential height composite alone (circles) and the combination of the events' geopotential height and precipitable water composite (diamonds) for all seven regions. CSI is the gray contours. This measure of skill is similar to the ETS value used, without the subtraction of chance hits.

patterns, while statistically significant, are not unique to our events. The strength of the synoptic connection of regional extreme precipitation events is low when using 500-hPa geopotential heights alone, seen by low conditional probabilities of an event occurring and near-zero values of ETS. When using both drivers, the composites of 500-hPa geopotential height and precipitable water, the conditional probability of an event occurring with similar patterns increases and ETS stays near-zero, as seen in Table 3. Yet all conditional probabilities, using our event composites, show an improvement from climatology.

To compare skill for all regions, a performance diagram is used (Fig. 6). All regions have low skill; therefore, synoptic characteristics seen during events are not unique to our extreme precipitation events. The skill metric used for the performance diagram is the critical success index (CSI), which may result in a higher skill value than the ETS seen in Table 3. This is due to the adjustment for chance hits that is seen in ETS; all equations can be found in the online supplemental material. The WC has the highest level of skill, with the highest conditional probability of an event occurring with similar synoptic characteristics: 26.6%. Therefore, WC events tend to look more similarly to the extreme event composites, than other regions. The NP has the lowest conditional probabilities (<7%) when compared with the other regions because of the low number of events within the region. Overall, the use of both drivers did result in small improvements than with geopotential height alone for all regions.

c. *Extreme precipitation event impacts*

During the PRES^{2}iP workshop hosted in the summer of 2018, stakeholders stressed the need to fully understand the impacts of extreme precipitation events (VanBuskirk et al. 2021). Although there might be an extreme amount of precipitation, it might not result in impacts on the ground. Therefore, here we present the impacts of these events in order to be confident that the events found are impactful for the regions. Storm reports found in the remaining four regions, NE, GL, NP, and MW, can be found in Figs. S3–S6 of the online supplemental material.

1) SOUTHEAST

Storm reports within events in the SE vary greatly, as seen in Fig. 7a. The SE has both convective storm reports (thunderstorm wind, tornado, hail, and lightning) and winter storm reports (winter weather, winter storm, heavy snow, and ice storm), this is similar to what is seen for the NE (Fig S6 in the online supplemental material). Impacts related to convection occurred the most with over 3000 reports of hail for all events within the SE from 1996 to 2018. Tropical storm reports also appear within the storm reports, which suggests there is

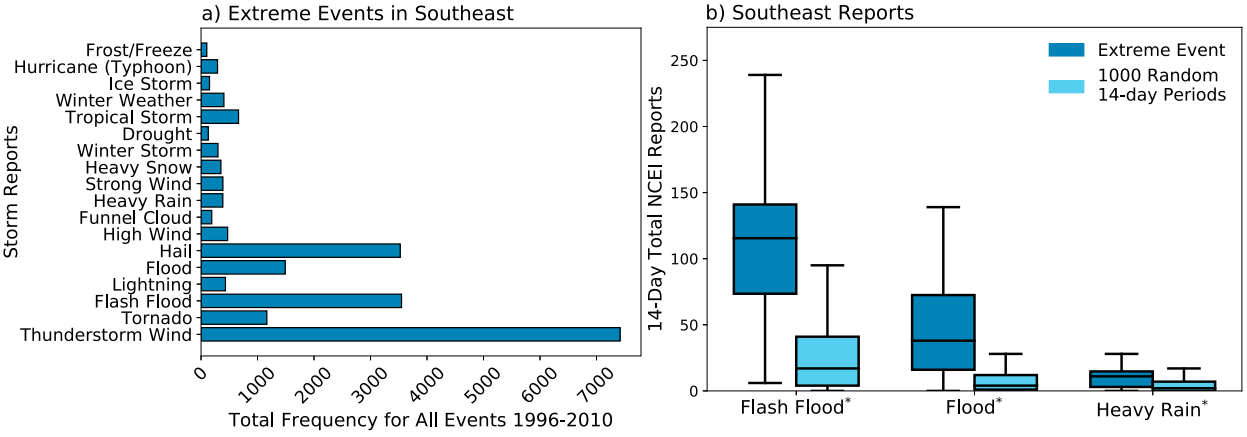

FIG. 7. (a) All NCEI storm reports from our extreme event days in the SE from 1996 to 2018. All reports that had less than 100 total counts are not shown. (b) Distribution of NCEI storm reports from 1996 to 2018 for flash flood, flood, and heavy rainfall for events in the SE (dark blue) and 1000 random 14-day periods excluding our extreme event days (light blue). Significant difference is found using a permutation test at $p < 0.1$, indicated as an asterisk next to the storm report labels along the x axis.

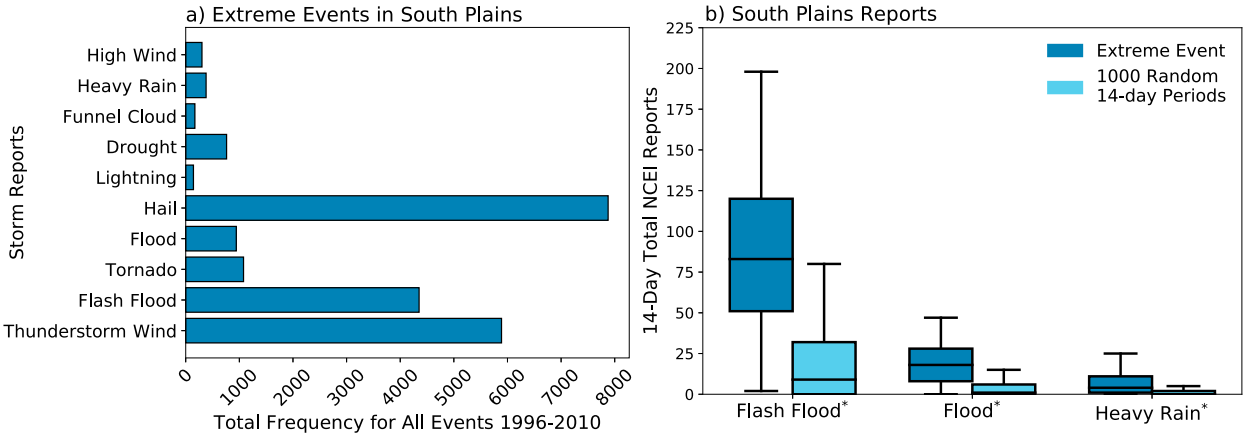

FIG. 8. As in Fig. 8, but for SP.

tropical storm activity during events in the SE. These are examined further in section 3c(4). This follows given that events happen throughout the year (Fig. 3) and therefore would create a vast range of impacts on the ground. When comparing events with random 14-day periods, we observe a significant increase in the number of flash flood, flood, and heavy rainfall events in SE, as seen in Fig. 7b. Events within the SE had anywhere from 75 to 125 flash flood reports per event; in random 14-day periods, this average drops to 20 reports. The SE also see an average of near 50 flood reports during the events, which indicates both flooding and flash flooding is common within SE events.

2) SOUTHERN PLAINS

All except three events within the SP occurred during the typical wet season of the region, from April to October. The SP is known for warm-season MCS producing large amounts of rainfall (Schumacher and Johnson 2006). In Fig. 8a it is shown that events in the SP produce many storm reports that are associated with convective systems, such as hail, thunderstorm wind, tornado, and lightning. Similar to the SE, the SP has a large amount of hail reports, with over 7500 reports, as well as tropical storm reports. Given that most events within the SP occur during the warm season, it follows that convective reports occur frequently during events. Further, there is a significant increase in reports of flash flood, flood, and heavy rainfall during events in comparison with nonevent periods (Fig. 8b). The average number of flash flood reports for a SP event is over 75 reports, and the average for flash flood during random 14-day periods is near 10 reports. This shows that events in the SP are more likely to produce large amounts of rainfall in a short amount of time rather than rainfall that would result in a report of a flood, despite the fact this precipitation is related to a 14-day event.

3) WEST COAST

Given that all WC events occur during the boreal winter, more winter precipitation storm reports are seen (Fig. 9a). Along with the typical reports of flood, flash flood, and heavy rain, we also see winter storm and heavy snow. The large number of heavy snow reports seen in WC events, over 1500 for all events, would indicate very different impacts than what is

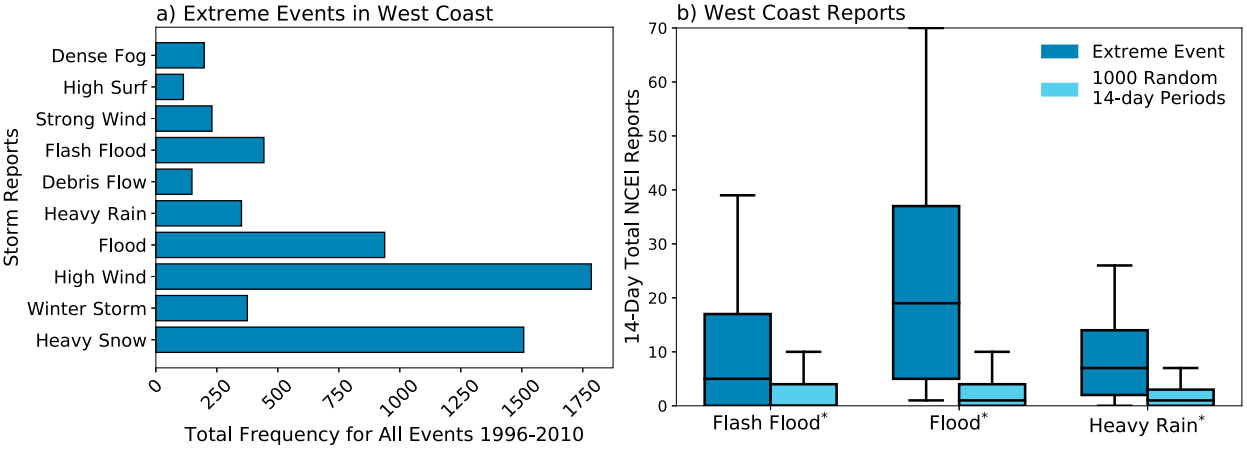

FIG. 9. As in Fig. 8, but for WC.

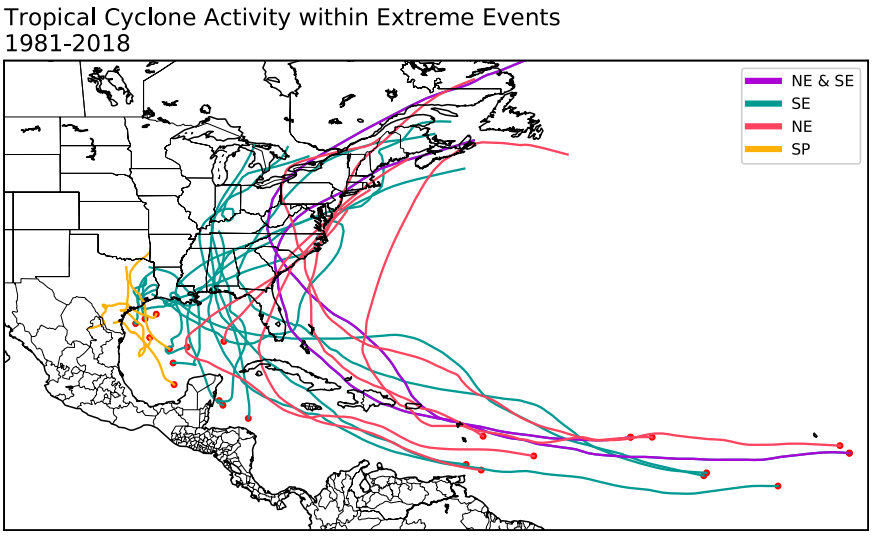

FIG. 10. Tracks of tropical cyclones that occurred during our extreme events in the SE (green), NE (orange), and SP (yellow), along with the two cyclones seen in both SE and NE events (purple).

seen within the SE and SP. A statistically significant difference between the event reports of flash flood, flood, and heavy rain and nonevents was also seen within the WC. The average number of flood reports within a WC extreme event is near 20 reports in a single event. During random nonevents, report totals for flood, flash flood, and heavy rainfall are below 5, as seen in Fig. 9b. This differs from report totals from the SE and SP, which both have more flash flooding reports than flood reports.

4) TROPICAL CYCLONE IMPACTS

To examine tropical cyclone (TC) influence, the International Best Track Archive for Climate Stewardship (IBTrACS) was used to find all tropical cyclone activity within events. Any event day that has a TC within the region is considered to be a TC-affected day. There was limited TC activity within events. This is most likely due to the constraint that the heaviest precipitation day and the surrounding two days cannot exceed 50% of the 14-day total precipitation, which limits the amount of TC activity seen the events. Removal of TC activity (events or days) did not result in changes to event composites used in finding synoptic connections. For each event with TC activity, the percent of total event rainfall that fell during the TC days was found. This gives an estimation of the contribution of the total precipitation from the TC days. All TCs tracks that are seen within events are shown in Fig. 10. The SE had the most TC activity with 10 events, 21.7% of SE events, occurring when a TC was within the region. There are some events within the NE and SE that have multiple TCs that occur during a singular event. For example, an SE event that started on 28 August 1988 had at least four days of TC activity from Hurricanes Chris and Florence. These four days accounted for 34.8% of the total event rainfall. If the precipitation was distributed evenly throughout all 14 days, we would expect 4 event days to make up 28.6%. Therefore, the TC activity likely provided a larger contribution of the overall precipitation for this event. Seven of the 10 SE events affected by TCs have TC days that make up at least 25% of the overall precipitation. Within the NE, 6 events had TC activity within them, 15.8% of NE events. In the SP, there was TC activity in only 4 events, 7.0% of SP events, although three of these events had higher amounts of daily precipitation on TC affected days than the remaining event days.

4. Discussion and conclusions

In this study, we extended an existing database of 14-day extreme precipitation events created by Jennrich et al. (2020). We found that with the addition of 2010–18 the overall monthly distribution of events does not change and the yearly distribution shows an increased number of events at the end of the time period. By splitting the Great Plains into the SP and the NP, we found very few events in the NP and the highest number of events in the SP. This might be due to the area threshold used for the NP in the event classification algorithm; since the NP is the smallest of all the regions, it would be more difficult for precipitation in the region to surpass this threshold. The typical timing of events is unique to each region. The NE, GL, NP, and SP all have a wet season during the warm months, whereas the MW and WC have a wet season during the cool months; the SE experiences precipitation throughout the entire year.

As in Jennrich et al. (2020), composites of all event-day standardized 500-hPa geopotential height anomalies from 1981 to 2018 showed a statistically significant trough/ridge dipole that is oriented over the region. Connections of the extreme events and their corresponding synoptic conditions was analyzed by using a 14-day sliding window from 1981 to 2018 to compare event periods with nonevent periods. The standardized 500-hPa height anomaly composite from every 14-day window was found and then compared with the extreme event

composite for the region using the congruence coefficient. Using 500-hPa geopotential heights alone resulted in very low skill of detecting the event periods. Regions had a conditional probability of an event to occur, given that the period was above the threshold, ranging from 6.6% in the NP to 19.9% in the WC. This highlights the low number of event periods above the threshold, as well as the large number of nonevent periods that have similar 500-hPa geopotential height patterns without extreme precipitation. The conditional probability of an event occurring, given that the period is below the threshold, had a much smaller range from 1.1% in the NP and 5.1% in the SP. This smaller range is due to the large number of nonevent periods below the threshold. Therefore, event periods can have a height field that differs greatly from the event-day composites even with significant anomalies, which presents a challenge for prediction of 14-day extreme precipitation using 500-hPa geopotential height alone.

Although 500-hPa geopotential heights may play a role in the formation of precipitation, geopotential heights alone are not a good predictor of extreme rainfall events. Therefore, standardized geopotential heights anomalies and standardized precipitable water were investigated together. Both fields were required to pass a CC threshold of 0.35 to be considered as similar to the extreme event composite. The conditional probability of an event to occur, given that it is above the threshold, increased in all regions to a range of 7.7%–26.6%, with the inclusion of precipitable water. This increase was due to the reduction of nonevent periods above the threshold. The conditional probability of an event to occur, given that it is below the threshold, only increased minimally in all regions. The WC has the highest skill, which indicates that WC events may be more synoptically driven than other regions, with similar patterns as seen in the extreme event composites. The composites of 500-hPa geopotential height and precipitable water show a strong signal for water transport into the region, similar to atmospheric rivers, which are a known source for extreme precipitation, and associated impacts, within the WC (Ralph et al. 2019). Other regions, such as the SP, SE, NP, MW, and NE, had many more convective impacts in the NCEI reports, with weak synoptic connections. The number of convective reports seen within these regions events may indicate that, although it is a 14-day event, the events may be made up of smaller convective, or mesoscale, storm systems. Overall, the synoptic connections, using extreme event composites, of 14-day events are weak, with low skill in discerning between event and nonevent periods.

During the PRES^{2}iP workshop hosted in June 2018, decision-makers stressed that, when defining an extreme event, impacts must be analyzed (VanBuskirk et al. 2021). Although all economic impacts of the events are difficult to define, potential impacts were found using NCEI storm reports. Storm reports give a good approximation to impacts that may been seen within the region during the 14-day event. Since event reports were only counted during the 14-day event, some flooding reports associated with event precipitation that occurred after the 14-day period may be missed. Still, all regions have significantly more flood reports when compared with random nonevents. Reports showed a wide variety of storm impacts throughout all regions. Within the NE, SE, GL, NP, SP, and MW we saw convective style storm reports such as hail, lightning, and thunderstorm wind. The NE, GL, MW, and WC also have winter weather storm reports from their events. All of these reports may result in impacts that may affect the region.

To discern the role of tropical cyclone activity within the events, we investigated the influence of TC precipitation on the event precipitation totals. The only regions that have TC activity within their events are the SP, SE, and the NE. It was found that overall, TC activity within the SP is minimal with only 4 total events affected, 7.0% of SP events. There is a larger influence of TCs within the SE and NE where 21.7% and 15.8%, respectively, of events had TC activity. There were three SE events that had more than 50% of the event rainfall occurring during TC days. For example, there were five TC days in a 1985 SE event, associated with Hurricane Juan, that produced 66.8% of the events precipitation. Therefore, TCs can be an important cause of extended precipitation extremes within the SE. TC activity within events is important to understand, not only to help isolate patterns associated with midlatitude precipitation, but also to highlight possible impacts of the events.

As a part of the PRES^{2}iP project, an extended database of S2S extreme precipitation events was recently created without the use of regional borders (Dickinson et al. 2021). This process objectively finds event regions after the creation of the database. Going forward, this database will be analyzed for predictability, in order to find common large-scale characteristics of S2S extreme precipitation events. Within this study, we use regional division to find extreme precipitation events within seven regions. The number of events found may be limited as a result of setting latitude/longitude boundaries prior to finding the events. If an event occurs over a regional division, it may not be seen as an event due to its reduced size. This also creates "hot spots" for high event counts within the center of the regions because of the low number of events happening near the boundaries, as seen in Fig. 1. The large size of the regions might also limit the strength of any synoptic connections because of the increase of climatic variability with increasing region size. Despite the large size, skill is still seen, which is encouraging for future prediction.

Into the future, there is still much to learn about predictability of these events. Although geopotential heights and moisture are a good foundation for synoptic connections for these events, there are many more driving factors to consider. For example, 200-hPa zonal winds, moisture flux, sea surface temperature, soil moisture, and evaporation could be analyzed in a similar fashion to find other important drivers of 14-day extreme precipitation events that may happen before or during the events. Investigating these events within seasonal models is required to reveal important characteristics about how these events may or may not be forecast to occur, for example, whether the same synoptic conditions found within event observations can lead to extreme precipitation in the models. Finding direct economic impacts of extreme events could help decision-makers to understand the best way

to create a more resilient population against extreme precipitation events.

Acknowledgments. The authors thank Dr. Renee McPherson, Dr. Jason Furtado, and the other members of the PRES^{2}iP team for their guidance and support with this study. We also thank the three anonymous reviewers for their feedback and edits that helped to improve this study. This work was supported by the National Science Foundation under their Prediction of and Resilience against Extreme Events (PREEVENTS) program, Grant ICER-1663840.

Data availability statement. The database of 14-day extreme precipitation events for the seven regions across the CONUS is available upon request to the authors. PRISM daily precipitation data are provided by PRISM Climate Group (http://www.prism.oregonstate.edu/). ERA5 data were downloaded from the Copernicus Climate Data Store (https://cds.climate.copernicus.eu/).

REFERENCES

Barlow, M., and Coauthors, 2019: North American extreme precipitation events and related large-scale meteorological patterns: A review of statistical methods, dynamics, modeling, and trends. *Climate Dyn.*, **53**, 6835–6875, https://doi.org/10.1007/s00382-019-04958-z.

Brunet, G., and Coauthors, 2010: Collaboration of the weather and climate communities to advance subseasonal-to-seasonal prediction. *Bull. Amer. Meteor. Soc.*, **91** 1397–1406, https://doi.org/10.1175/2010BAMS3013.1.

Copernicus Climate Change Service, 2017: ERA5: Fifth generation of ECMWF atmospheric reanalyses of the global climate. Copernicus Climate Change Service Climate Data Store, accessed 20 July 2020, https://cds.climate.copernicus.eu/.

Curriero, F. C., J. A. Patz, J. B. Rose, and S. Lele, 2001: The association between extreme precipitation and waterborne disease outbreaks in the United States, 1948–1994. *Amer. J. Public Health*, **91**, 1194–1199, https://doi.org/10.2105/AJPH.91.8.1194.

Daly, C., M. Halbleib, J. I. Smith, W. P. Gibson, M. K. Doggett, G. H. Taylor, J. Curtis, and P. P. Pasteris, 2008: Physiographically sensitive mapping of climatological temperature and precipitation across the conterminous United States. *Int. J. Climatol.*, **28**, 2031–2064, https://doi.org/10.1002/joc.1688.

Dickinson, T. A., M. B. Richman, and J. C. Furtado, 2021: Subseasonal to seasonal extreme precipitation events in the contiguous united states: Generation of a database and climatology. *J. Climate*, **34**, 7571–7586, https://doi.org/10.1175/JCLI-D-20-0580.1.

Flanagan, P. X., J. B. Basara, J. C. Furtado, and X. Xiao, 2018: Primary atmospheric drivers of pluvial years in the United States Great Plains. *J. Hydrometeor.*, **19**, 643–658, https://doi.org/10.1175/JHM-D-17-0148.1.

Furl, C., H. Sharif, J. W. Zeitler, A. E. Hassan, and J. Joseph, 2018: Hydrometeorology of the catastrophic Blanco River flood in south Texas, May 2015. *J. Hydrol. Reg. Stud.*, **15**, 90–104, https://doi.org/10.1016/j.ejrh.2017.12.001.

Groisman, P. Ya., R. W. Knight, and T. R. Karl, 2012: Changes in intense precipitation over the central United States. *J. Hydrometeor.*, **13**, 47–66, https://doi.org/10.1175/JHM-D-11-039.1.

Jennrich, G. C., J. C. Furtado, J. B. Basara, and E. R. Martin, 2020: Synoptic characteristics of 14-day extreme precipitation events across the United States. *J. Climate*, **33**, 6423–6440, https://doi.org/10.1175/JCLI-D-19-0563.1.

Karl, T. R., and R. W. Knight, 1998: Secular trends of precipitation amount, frequency, and intensity in the United States. *Bull. Amer. Meteor. Soc.*, **79**, 231–242, https://doi.org/10.1175/1520-0477(1998)079<0231:STOPAF>2.0.CO;2.

Kunkel, K. E., S. A. Changnon, and J. R. Angel, 1994: Climatic aspects of the 1993 upper Mississippi River basin flood. *Bull. Amer. Meteor. Soc.*, **75**, 811–822, https://doi.org/10.1175/1520-0477(1994)075<0811:CAOTUM>2.0.CO;2.

——, K. Andsager, and D. R. Easterling, 1999: Long-term trends in extreme precipitation events over the conterminous United States and Canada. *J. Climate*, **12**, 2515–2527, https://doi.org/10.1175/1520-0442(1999)012<2515:LTTIEP>2.0.CO;2.

Livneh, B., E. Rosnberg, C. Lin, B. Nijssen, V. Mishra, K. Andreadis, E. Maurer, and D. Lettenmaier, 2013: A long-term hydrologically based dataset of land surface fluxes and states for the conterminous United States: Update and extensions. *J. Climate*, **26**, 9384–9392, https://doi.org/10.1175/JCLI-D-12-00508.1.

Mastrantonas, N., L. Magnusson, F. Pappenberger, and J. Matschullat, 2022: What do large-scale patterns teach us about extreme precipitation over the Mediterranean at medium- and extended range forecasts? *Quart. J. Roy. Meteor. Soc.*, **148**, 875–890, https://doi.org/10.1002/qj.4236.

Miller, S., R. Muir-Wood, and A. Boissonnade, 2008: An exploration of trends in normalized weather-related catastrophe losses. *Climate Extremes and Society*, Cambridge University Press, 225–247, https://doi.org/10.1017/CBO9780511535840.015.

Murphy, J. D., 2018: Storm data preparation. National Weather Service Instruction 10-1605, 110 pp., https://www.nws.noaa.gov/directives/sym/pd01016005curr.pdf.

NCEI, 2008: State of the climate: National Climate Report for annual 2007. NOAA, accessed 19 October 2020, https://www.ncdc.noaa.gov/sotc/national/200713.

——, 2019: U.S. billion-dollar weather and climate disasters. NOAA, https://www.ncdc.noaa.gov/billions/.

——, 2020: Storm Events Database. NOAA, accessed 3 February 2020, https://www.ncdc.noaa.gov/stormevents/.

Pan, B., K. Hsu, A. AghaKouchak, S. Sorooshian, and W. Higgins, 2019: Precipitation prediction skill for the West Coast United States: From short to extended range. *J. Climate*, **32**, 161–182, https://doi.org/10.1175/JCLI-D-18-0355.1.

PRISM Climate Group, 2004: Northwest alliance for computational science and engineering. Oregon State University, http://prism.oregonstate.edu.

Ralph, F. M., J. J. Rutz, J. M. Cordeira, M. Dettinger, M. Anderson, D. Reynolds, L. J. Schick, and C. Smallcomb, 2019: A scale to characterize the strength and impacts of atmospheric rivers. *Bull. Amer. Meteor. Soc.*, **100**, 269–289, https://doi.org/10.1175/BAMS-D-18-0023.1.

Richardson, D., R. Neal, R. Dankers, K. Mylne, R. Cowling, H. Clements, and J. Millard, 2020: Linking weather patterns to regional extreme precipitation for highlighting potential flood events in medium- to long-range forecasts. *Meteor. Appl.*, **27**, e1931, https://doi.org/10.1002/met.1931.

Robertson, A. W., A. Kumar, M. Peña, and F. Vitart, 2015: Improving and promoting subseasonal to seasonal prediction. *Bull. Amer. Meteor. Soc.*, **96**, ES49–ES53, https://doi.org/10.1175/BAMS-D-14-00139.1.

Schumacher, R. S., and R. H. Johnson, 2006: Characteristics of U.S. extreme rain events during 1999–2003. *Wea. Forecasting*, **21**, 69–85, https://doi.org/10.1175/WAF900.1.

Sharma, S., and Coauthors, 2017: Eastern U.S. verification of ensemble precipitation forecasts. *Wea. Forecasting*, **32**, 117–139, https://doi.org/10.1175/WAF-D-16-0094.1.

Slater, L. J., and G. Villarini, 2016: Recent trends in U.S. flood risk. *Geophys. Res. Lett.*, **43**, 12 428–12 436, https://doi.org/10.1002/2016GL071199.

Son, S.-W., H. Kim, K. Song, S.-W. Kim, P. Martineau, Y.-K. Hyun, and Y. Kim, 2020: Extratropical prediction skill of the subseasonal-to-seasonal (S2S) prediction models. *J. Geophys. Res. Atmos.*, **125**, e2019JD031273, https://doi.org/10.1029/2019JD031273.

United Nations, 2015: The human cost of weather-related disasters 1995–2015. UNISDR Rep., 30 pp., http://www.unisdr.org/2015/docs/climatechange/COP21_WeatherDisastersReport_2015_FINAL.pdf.

VanBuskirk, O., P. Cwik, R. A. McPherson, H. Lazrus, E. Martin, C. Kuster, and E. Mullens, 2021: Listening to stakeholders: Initiating research on sub-seasonal to seasonal heavy precipitation events by first understanding what users need. *Bull. Amer. Meteor. Soc.*, **102**, E1972–E1986, https://doi.org/10.1175/BAMS-D-20-0313.1.

Vitart, F., and Coauthors, 2017: The subseasonal to seasonal (S2S) prediction project database. *Bull. Amer. Meteor. Soc.*, **98**, 163–173, https://doi.org/10.1175/BAMS-D-16-0017.1.

Zhao, S., Y. Deng, and R. X. Black, 2017: A dynamical and statistical characterization of U.S. extreme precipitation events and their associated large-scale meteorological patterns. *J. Climate*, **30**, 1307–1326, https://doi.org/10.1175/JCLI-D-15-0910.1.